PAPER • **OPEN ACCESS**

Spray combustion characteristics of effervescent atomizer inside experimental furnace

To cite this article: Safwat A. Wilson *et al* 2019 *IOP Conf. Ser.: Mater. Sci. Eng.* **610** 012087

View the article online for updates and enhancements.

This content was downloaded from IP address 195.43.0.86 on 12/09/2021 at 09:30

Spray combustion characteristics of effervescent atomizer inside experimental furnace

Safwat A. Wilson[1], Gaber M. Asar[2], Eslam M. Elshahawy[3]

Mechanical Power Eng. Dept., Faculty of Engineering, Menoufia University, Egypt

* Corresponding author [1]. Tel.: 002-01148877606. E-mail address: safwatwilson@yahoo.com
Author [2]. gasar2001@yahoo.com Author [3]. es-lam@live.com

Abstract. The spray combustion characteristics of "inside-out" effervescent atomizer at low injection pressure have been investigated in the present study. The atomizer is mounted on experimental furnace cooled by separate segments water jacket the plain orifice atomizer is powered by diesel fuel and air as atomizing gas. The study shows the influence of A/F ratio, atomizing gas to liquid mass ratio (GLR), injection pressure, and exit orifice diameter on flame temperature distribution inside the furnace. cooling water heat flux, stack temperature, and combustion efficiency. The air to fuel mass ratio (A/F) varies from 20 to 50 Kg_{air}/Kg_{fuel}, and operating pressure varies from 0.5 to 2 bar. The results show that the increasing on A/F ratio decreases the flame length, and exhaust gas temperature, while the combustion efficiency increases. It was found also that, when using A/F ratios higher than 30 the combustion efficiency becomes greater than 90%. Where, the increasing on operating pressure increases the flame maximum temperature and heat transfer to cooling water. Moreover, increasing the combustion efficiency. The results could enrich our knowledge of effervescent spray combustion characteristics and achieving higher combustion efficiency with low pollutant emissions.

Keywords: Twin-fluid; Effervescent atomizer; Flame temperature distribution; Combustion efficiency.

Nomenclature

GLR	Gas to liquid mass ratio	[%]	ρ	Density	[Kg/m^3]
P_{inj}	Injection pressure (g)	[bar]	σ	Surface tension	[N/m]
L	length of exit orifice	[mm]	μ	Viscosity	[Kg/m.s]
D	Orifice exit diameter	[mm]	R	Combustor radius	[mm]
η_c	Combustion efficiency	[%]	UHC	Unburned hydrocarbons	
Qw/A_s	Cooling water heat flux	[Kj/hr. m^2]	A/F	Air to fuel mass ratio	[Kg_{air}/Kg_{fuel}]
CO	Carbon monoxide		Cp_w	Specific heat of water	[Kj/Kg.K]

1. Introduction

Liquid atomization is a process of great importance in many applications. Today, liquid hydrocarbon fuels contribute a great amount of the energy source, due to its flexibility in of transporting and storing. However, liquid fuels cannot be used in their bulky form. Therefore, in most of the applications the liquid fuel is mixed with the oxidizer and burned in the form of sprays of small size droplets. This type of combustion is

Content from this work may be used under the terms of the Creative Commons Attribution 3.0 licence. Any further distribution of this work must maintain attribution to the author(s) and the title of the work, journal citation and DOI.
Published under licence by IOP Publishing Ltd

relevant to a variety of the fuel systems. Hence, for developing these systems, and understanding of the basic physical processes related to spray combustion for increasing energy production and reducing pollutant emissions of fuel combustion. Therefore, great efforts are applied by the mechanical engineers in the world to investigate, develop, and then control the combustion processes and systems with the associated phenomena.

In the present study, the spray and combustion characteristics produced by an effervescent atomizer is investigated experimentally at different designs and operating conditions for achieving clean combustion with high efficiency and low pollutants. Using a modern technique of fuel atomization "effervescent atomization". This method of atomization has been shown to produce well-atomized sprays with only a small amount of aerating gas at relatively low injection pressures [1]. It has been shown to work well even with liquids of high viscosity (Bio-fuel) [2].

Effervescent atomizer uses gas injection into the liquid to form bubbles in the mixing chamber. The gas and liquid mixture move downstream towards the exit orifice. The bubbles inside the liquid flow enhances the atomization process by decreasing the amount of the liquid passing through the exit orifice and by the expansion of the bubbles inside the liquid after spouting the exit orifice due to a sudden pressure drop. The expansion of bubbles forms thin ligaments and small droplets [3]. The aim of liquid fuel atomization is enhancing the evaporation rate to ensure good mixing of the fuel vapor with air before reaching the flame zone.

Studies of spray combustion are categorized into two major trends: the first is based on analyzing the real combustion process, starting from single fuel droplet combustion. The present work carried out by applying the second trend; direct observations of spray combustion are made to investigate the different accompanying phenomena such as flame length, heat transfer, flame stability, and combustion efficiency.

Lian et al. [4] carried out an experimental study on the spray combustion produced by effervescent atomizer. A cylindrical furnace was used to investigate diesel oil spray flame systematically in swirling air flow. Cooling water heat transfer and mass transfer processes among vortexes induce flame propagation. The volume fractions of carbon monoxide (CO) and hydrocarbon (HC) in exhaust gases decrease gradually with the increasing of excess air and air/liquid mass flow rate ratio (GLR). The exhaust gas recirculation (EGR) reduces the nitrogen oxides by 30%. The air swirl intensity has distinct effects on spray flame structure [5].

Onuma et al. [6] compared the flame characteristics of kerosene spray burning and turbulent gas (propane) diffusion. They burnt with the same combustion air velocity in a vertical cylindrical furnace. Temperature distributions and exhaust gas composition were measured in the flame of an air-atomizing burner. It was observed that most of the droplets in the flame do not burn individually, but that fuel vapor from the droplets concentrates and burns like a gaseous diffusion flame.

Okasha et al. [7] performed an experimental study using a vertical cylindrical water-cooled combustor. The flame stability and combustion efficiency were obtained over wide ranges of (A/F) ratios, and at different percentages of olive-cake in the diesel fuel. It was noticed that the rate of heat transfer to the water jacket of the combustor and the combustion efficiency is improved when the percentage of olive-cake in the diesel fuel is increased to 7 wt % [8,9].

Akinyemi et al. [10] studied the combustion of diesel, and vegetable oil utilizing a twin-fluid atomizer. The results showed that the injector produced clean blue flames signifying mainly premixed combustion for the fuels. Low emissions of CO and NO_x are achieved for the two fuels consistently showing the excellent combustion performance of the injector [11].

The importance of spray quality is a key parameter in combustion applications, as it directly affects gaseous and particulate emissions. Incomplete combustion characterized by increased CO levels is a typical example of the possible consequences [12,13]. To enhance fuel combustion efficiency, use of fuel injectors which produce uniform circumferential and radial temperature patterns will be required. The higher combustion temperatures will put a greater heat load on the combustor liners. Lyons et al. [14] investigate the influence of effervescent atomizer on gas turbine emissions and combustion efficiency. The results showed that increased temperatures and pressures will make the aircraft gas turbine more efficient.

Failure to achieve maximum values of combustion efficiency is generally considered unacceptable. Because The combustion efficiency is related to the amount of unburned hydrocarbon (UHC) and carbon monoxide (CO). The higher combustion efficiency the lower combustion emissions [15-19].
In literature, there is a lack of information about combustion characteristics and combustion efficiency of effervescent atomizer. Therefore, the main objective of the present study is to investigate the effect of spray and combustion characteristics of effervescent atomizer powered by diesel fuel in a horizontally positioned cylindrical furnace. Combustion efficiency and the effect of operating and design conditions on its performance will also be considered.

2. Experimental set-up

The test rig is constructed to facilitate the measurements of the flame characteristics (the flame structure and the flame temperature distribution, in addition to calculating combustion efficiency) of an effervescent atomizer. The test rig and auxiliary systems are schematically illustrated in figure 1. It consists of a horizontal small-scale cylindrical furnace connected to an effervescent atomizer installed through divergent cone that tied with air supply. The combustion air is supplied to the burner from a centrifugal blower. The combustion air flow rate is controlled through a globe valve and measured using a calibrated orifice meter. The effervescent atomizer used in the present work is a plain-orifice atomizer, made from steel and “inside-out" configuration, where the air is injected into the mixing chamber from the aerator. The diesel fuel surrounds the aerator as shown in the figure 2. The atomizer cross section area is cylindrical shape of 40 mm diameter. The internal diameter of the mixing chamber is 20 mm. The aerator is made from steel tube with 5mm inner diameter. A two air injection holes of 0.5 mm diameter were drilled at 5 mm from the aerator end. Three nozzle cups with different orifice diameters are used in the present experimental work. Orifice dimensions of the cups are given in the following table.

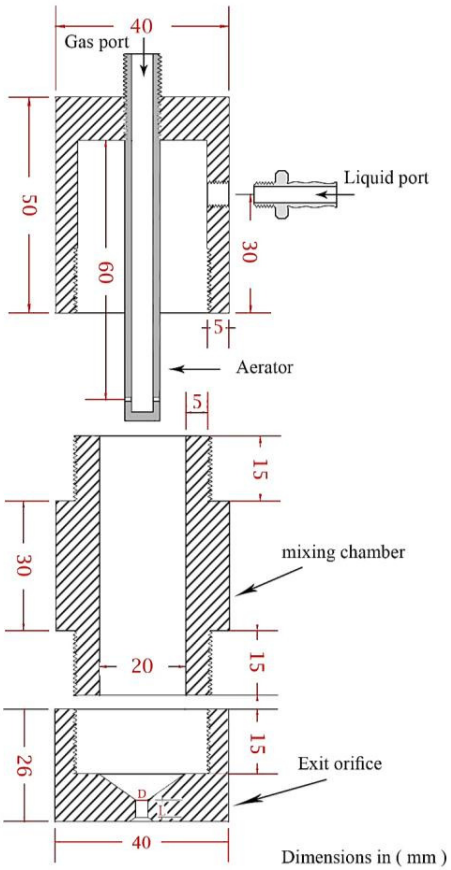

Figure 1. Schematic diagram of the tested effervescent atomizer.

D (mm)	L (mm)	L/D	θ º
1	5	5	45
2	5	2.5	45
3	5	1.67	45

The atomizer is supplied with air from large screw compressor equipped with large capacity air vessel. The atomizing air pressure is regulated through a pressure regulator and its flow rate is measured using a calibrated orifice meter. The combustion air flows through swirl generator (swirler) with blade angle 45º before the furnace entrance. The fuel is supplied from a tank pressurized by the compressed air. The air pressure to the fuel tank is regulated using a pressure regulator. The combustor is an insulated horizontal cylindrical water-cooled flame tube of 480 mm inner diameter and 1500 mm length. The cylindrical flame tube is cooled by a water circular jacket of 600 mm external diameter and is divided to 10 unequal segments. At the middle of each segment a radially aligned tap of 15 mm diameter is provided to allow the insertion of the different temperature measuring probes. At the bottom a main cooling water header is used for the distribution of the cooling water to each segment. The cooling water flow rate is measured using a calibrated orifice meter at

the inlet of each segment. The hot water leaves each segment at the top side and its temperature is measured using a thermocouple. The exhaust gas temperature is measured at combustor exit.

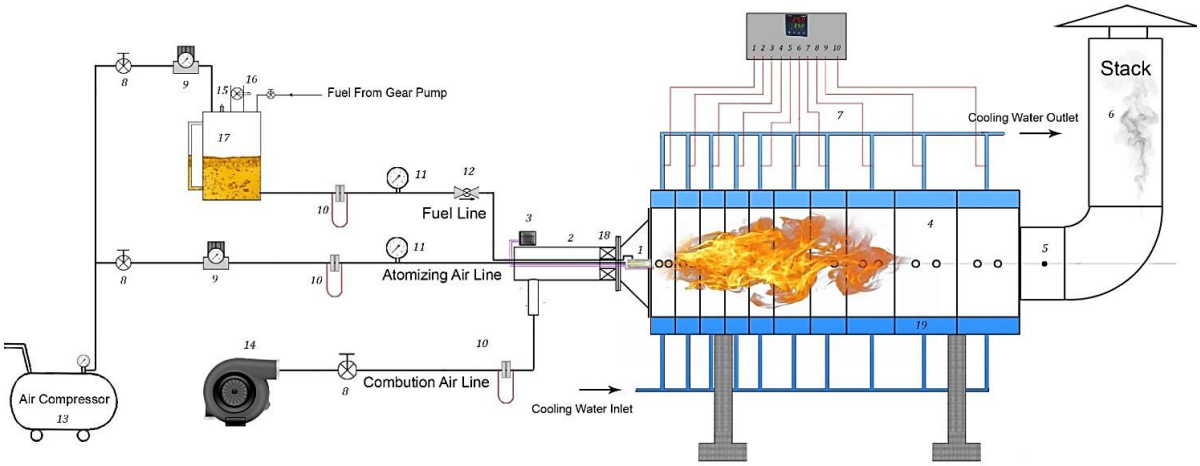

1- Effervescent Atomizer
2- Burner Tube
3- Electrical Ignitor Transformer
4- Horizontal Furnace
5- Stack Temperture Port
6- Emission Port
7- Thermocouple Type(t)
8- Control Valve
9- Pressure Regulator
10- Orifice Flow meter
11- Pressure Gauge
12- Check Valve
13- Air Compressor
14- Air Blower
15- Relief Valve
16- Filling Valve
17-Compressed Fuel Tank
18- Swirl Generator
19-Water Circular Jacket

Figure 2. schematic diagram of the experimental test rig

In any atomization process the spray characteristics are dependent on several parameters including liquid physical properties, atomizer internal geometry, and operating conditions. Table 1 summarizes the design and operating conditions used in the present study.

Run no.	*A/F*	*Injection pressure (g)*	*Atomizing Gas*	*Liquid*	*GLR*	*L/D*
Effect of Gas to liquid mass ratio (GLR)						
1	30	1.5 bar	Air	diesel	0.8 %	2.5
2	30	1.5 bar	Air	diesel	1 %	2.5
3	30	1.5 bar	Air	diesel	1.2 %	2.5
4	30	1.5 bar	Air	diesel	1.4 %	2.5
Effect of injection pressure (p_{inj})						
5	40	0.5 bar	Air	diesel	1 %	2.5
6	40	1 bar	Air	diesel	1 %	2.5
7	40	1.5 bar	Air	diesel	1 %	2.5
8	40	2 bar	Air	diesel	1 %	2.5
Effect of exit orifice length to diameter ratio (L/D)						
9	40	1.5 bar	Air	diesel	1 %	5
10	40	1.5 bar	Air	diesel	1 %	2.5
11	40	1.5 bar	Air	diesel	1 %	1.67
Effect of air to fuel ratio (A/F)						
12	20	1 bar	Air	diesel	1 %	2.5
13	30	1 bar	Air	diesel	1 %	2.5

14	40	1 bar	Air	diesel	1 %	2.5
15	50	1 bar	Air	diesel	1 %	2.5

Table 1. Design and operating conditions used in the present study.

Experimental errors associated with the present investigation result from a number of sources including systematic measurement errors, and errors arising from the fluctuations in operating parameters during each run. The most common sources of errors in the measured parameters are found in the pressure drop across orifice meter, flame temperature, and cooling water temperature. These parameters have direct effect on the accuracy of temperature and mass flow rates. Uncertainty of each parameter is shown in Table 2.

Parameter	***Uncertainty***	***Range***
Atomizing air mass flow rate	± 0.85 %	Up to 0.624 kg/hr
Fuel mass flow rate	± 1.11 %	Up to 16.5 kg/hr
Combustion air mass flow rate	± 0.16 %	Up to 350 kg/hr
Flame temperature	± 2.5 ˚C	1:1800 ˚C
Cooling water temperature	± 0.5 ˚C	1:100 ˚C

Table 2. Uncertainty and ranges of measured parameters.

3. Results and discussion

3.1 Influence of Air to Fuel Ratio (A/F)

The effect of air-to-fuel ratio on temperature distribution, heat transfer to the cooling water and combustion efficiency will be discussed in detail. Different air to fuel ratios is used by fixing diesel fuel flow rate and changing the air flow rate in all the experiments.

3.1.1 flame temperature distribution

Figure 3 shows the flame temperature distribution along the axis of the flame for different A/F ratios. The temperature distribution along the centerline of the furnace showed low temperature near the nozzle and then increases to the maximum temperature then decreases with moving downstream from the burner tip.

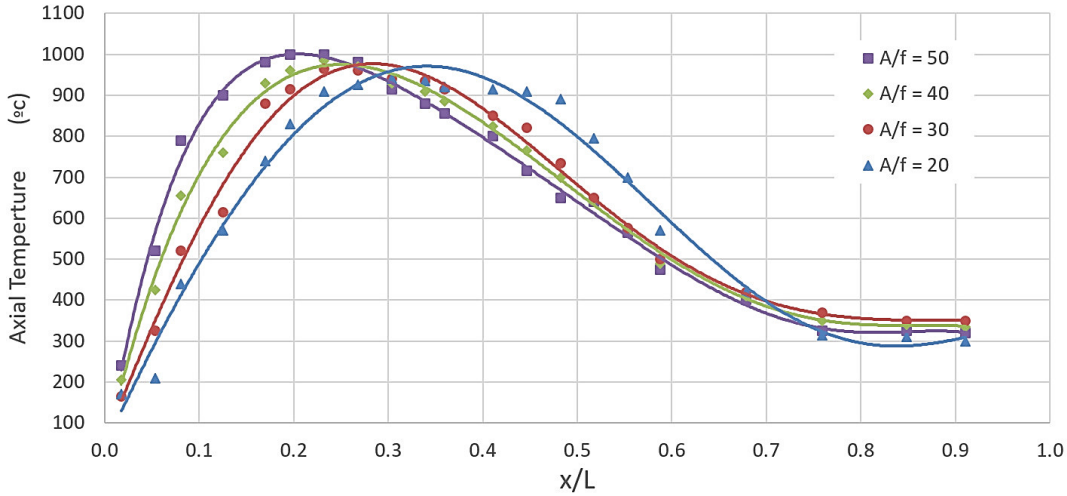

Figure 3 Influence of air to fuel ratio on flame temperature distribution along the axis at p_{inj} = 1 bar, GLR= 1 %, and L/D = 2.5

The high temperature is recorded where intense mixing among fuel, atomizing air, and combustion air streams with nearly stoichiometric mixture. It is found also that the maximum temperature of the flame is nearly 25 % relative to furnace length, at which the mixing of air and fuel is approximately completed. Further increase in A/F ratio decreases the flame length as well. Therefore, the increasing of A/F ratio shifting the maximum temperature towards the burner tip.

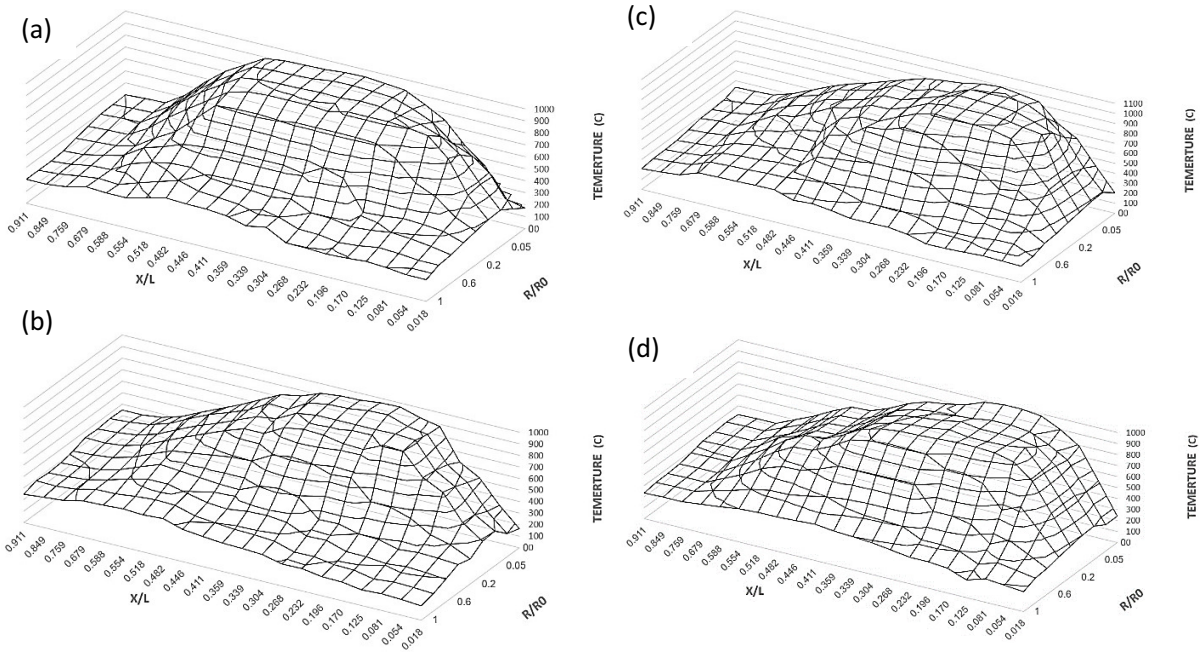

Figure 4. 3-D surface of flame temperature (^{o}c) in the combustor at GLR= 1 %, L/D= 2.5, and p_{inj} = 1 bar a) A/F= 20 b) A/F=30 c) A/F=40 d) A/F=50.

Figure 4(a-d) shows 3-D surface of flame temperature in the combustor at different A/F ratios (20,30,40 and 50 Kg_{air}/Kg_{fuel}). It can be seen that the flame length decreases with increasing air to fuel ratio and the maximum temperature moves toward burner tip. The fuel mass flux decreases with increasing radial distance and become more uniform with increasing axial distance downstream the atomizer. Therefore, the profile near the burner tip shows a high temperature at the flame zone and then a very low temperature at the center and then lower temperature at the other points farther than the center because of the flame diameter is small, subsequently the other points locate outer the flame zone. The temperature profile becomes uniform with increasing axial distance as this region represents the exhaust gas temperature outer the flame region.

3.1.2 Cooling Water Heat Flux

The heat flux to the water jacket of the furnace is calculated from the cooling water temperature measurements and mass flow rate for each segment according to the following expressions:

$$Q_w = \dot{m}_w \, C\mathrm{p}_w \, (T_{w,e} - T_{w,i})$$

$$\text{Heat flux} = \frac{\mathrm{Qw}}{\mathrm{A}_s}$$

Figure 5 shows heat flux for different values of air-to-fuel ratios. It is found that the heat flux profile in all cases increases to the maximum value then decreases with moving downstream from the burner tip. There is a good agreement between the temperature distribution in the combustor and the distribution of heat flux as shown in Figure 3. Decreasing of flame length with increasing air to fuel ratio beside the combustion air turbulence inside the furnace lead to increasing the heat transfer rate to cooling water.

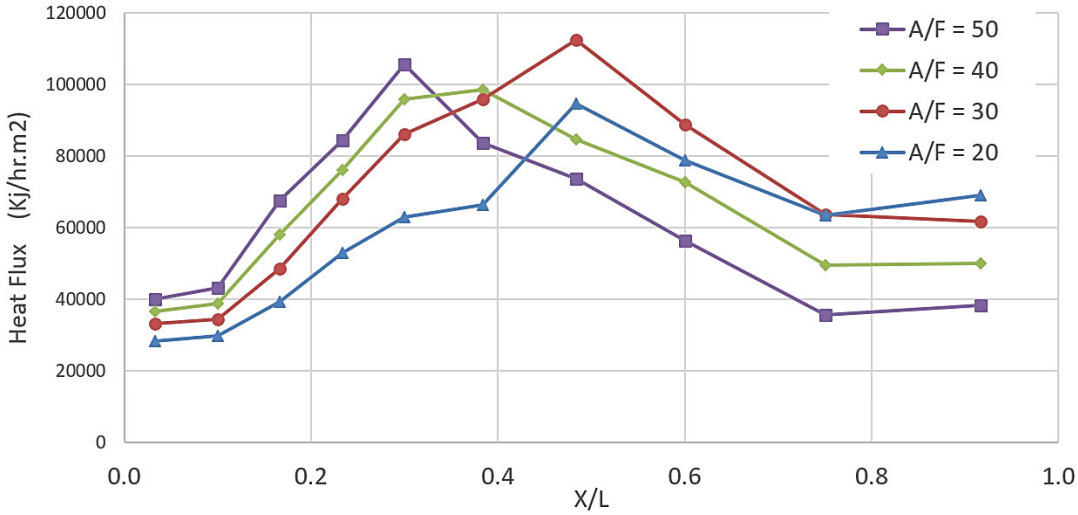

Figure 5. Total heat flux to the water jacket for different air to fuel ratio at GLR= 1 %, L/D= 2.5, and p_{inj} = 1 bar.

3.1.3 Stack Temperature

While stack temperature is considered as indirect measure of thermal efficiency, the present work interested with recording their values at different A/F. Figure 6 shows the relation between exhaust temperatures with different values of air- to-fuel ratios. It is observed that the exhaust temperature decreases with increasing air-to-fuel ratio up to 50. This decreasing is due to increasing the combustion air flow rate (leaner mixture). The excess air absorbs part of combustion energy and consequently exhaust temperature decreases.

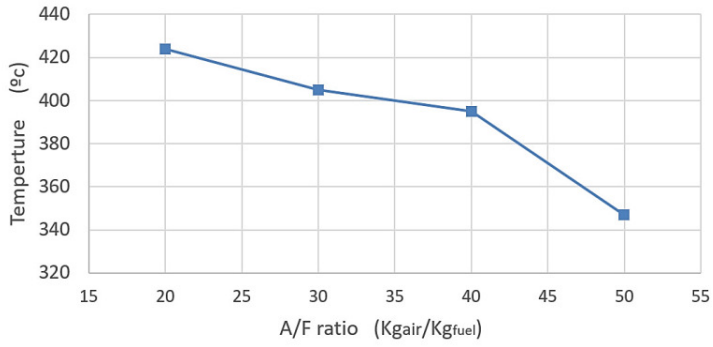

Figure 6. Stack temperature for different air to fuel ratio at GLR= 1 %, L/D= 2.5, and p_{inj} = 1 bar.

3.1.4 Combustion Efficiency

Figure 7 shows the influence of air to fuel ratio on combustion efficiency. The increasing on A/F ratio decreases the flame length. At low A/F ratio, the fuel needs to air to complete combustion. So, the flame stretches until all amount of fuel burned. The small amount of air leads to incomplete combustion and smoke appears with flame. Increasing of combustion air secures the necessary amount for complete combustion and non-smoke flame. Furthermore, the turbulence of combustion air makes good mixing of air with fuel and increases combustion rate. Therefore, the combustion efficiency increases at higher air to fuel ratios. The higher combustion efficiency achieves low emissions. Combustion efficiency is defined as:

η_c= (heat released in combustion) / (heat available in fuel)

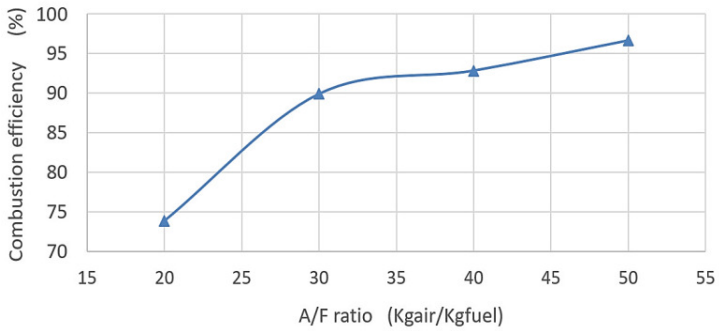

Figure 7. Influence of injection pressure on combustion efficiency at GLR= 1 %, L/D= 2.5, and p_{inj} = 1 bar.

3.2 Influence of Gas to Liquid Mass Ratio (GLR)

The atomizing gas-to-liquid ratio by mass (GLR) is an important operating parameter for atomization and spray characteristics since it is desirable to minimize the amount of atomizing gas supplied while maintaining a small mean drop size. In this section the effect of gas to liquid ratio (GLR) will be discussed in detail on flame temperature distribution, heat transfer to the cooling water and combustion efficiency.

3.2.1 Flame temperature distribution

Temperature distribution along furnace axis at different GLR appears clearly in Figure 8. During the experiments, gas to liquid ratios ranging from 0.8% to 1.4 %. While A/F, injection pressure and nozzle diameter are kept constant at 30, 1.5 bar, and 2 mm respectively. It is found that the peak temperature is recorded where intense mixing among fuel, atomizing air, and combustion air streams with nearly stoichiometric mixture. The maximum temperature of the flame is in range of 15% to 20 % relative to furnace length, at which the rate of reaction is relatively high. The increasing of GLR ratio decreases the flame length and widen the spray cone angle. Therefore, the increasing of GLR ratio leads to shifting the maximum temperature towards the burner tip.

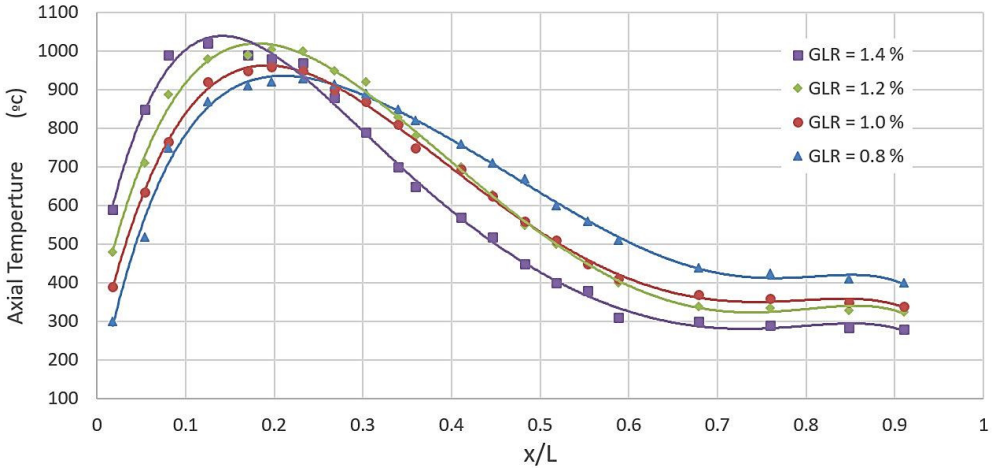

Figure 8. Influence of gas to liquid ratio on flame temperature distribution along the axis at A/F= 30 Kg_{air}/Kg_{fuel}, p_{inj} = 1.5 bar, and L/D = 2.5

A uniform temperature region almost occurs in the outer recirculation zone and the temperature declines outside the flame boundary. As the axial distance increases from the burner tip, the fuel mass flux become

more uniform. Subsequently, the temperature distribution become more uniform and flatter. Moreover, the increasing of GLR widen the spray cone angle with uniform mass distribution. At the end of furnace, the temperature difference disappear because of the measuring points are outside the flame zone. Figure 9(a-d) shows 3-D surface of flame temperature in the combustor at different gas to liquid ratios ranging from 0.8 % to 1.4 %, A/F= 30 kg_{air}/Kg_{fuel} and exit orifice diameter 2 mm. It can be seen that the flame length decreases with increasing gas to liquid ratio and the maximum temperature moves to burner tip.

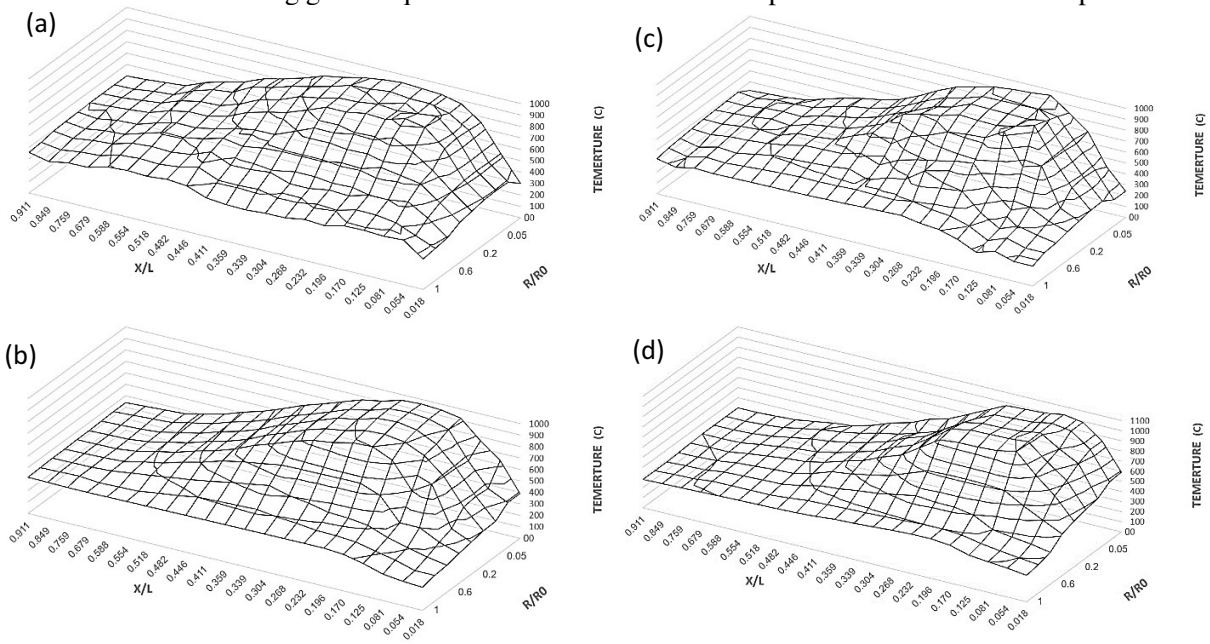

Figure 9. 3-D surface of flame temperature (°c) in the combustor at p_{inj} = 1.5 bar, L/D= 2.5, and A/F= 30 Kg_{air}/Kg_{fuel} a) GLR= 0.8% b) GLR= 1 % c) GLR= 1.2% d) GLR= 1.4%.

3.2.2 Cooling Water Heat Flux

The effect of GLR on heat transferred to the water jacket is recorded as shown in Figure 10. During the experiments, GLR is increased by increasing the fuel flow rate while the atomizing air is kept constant. It is found that the heat flux profile in all cases increases to the maximum value then decreases with moving downstream from the burner tip. It seems to take the same trend of the flame temperature distribution along the furnace centerline. The variation of fuel flow rate changes the amount of heat released in the combustor. Therefore, the increasing of GLR decreases the amount of heat transfer to the cooling water.

3.2.3 Stack Temperature

Figure 11 shows the relation between exhaust temperatures and different values of gas to liquid ratios. It is observed that the exhaust temperature decreases with increasing gas to liquid ratio. This decreasing is due to deceasing of flame length with increasing GLR. Moreover, the axial flame temperature at the end of the furnace give clear indication of exhaust gas temperature.

3.2.4 Combustion Efficiency

The combustion efficiency is related to the amount of unburned hydrocarbon (UHC) and carbon monoxide (CO). The higher combustion efficiency achieves low combustion emissions. Figure 12 shows the influence of gas to liquid ratio on combustion efficiency. The increasing of gas to liquid ratio widen the spray cone angle with more uniform fuel mass distribution. This increasing of GLR providing spray with fine drops and higher evaporating rate of the drops achieving combustion with short stable flame. Therefore, the combustion efficiency increases at higher GLRs.

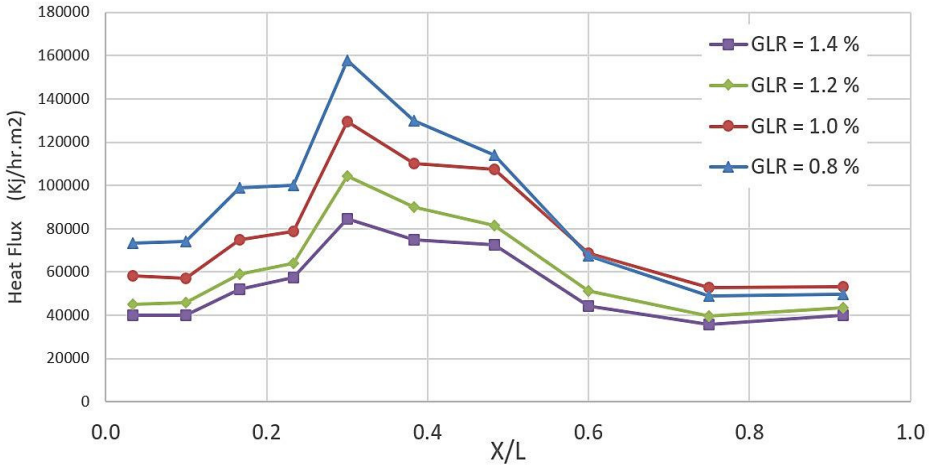

Figure 10. Total heat flux to the water jacket for different gas to liquid ratios at p_{inj} = 1.5 bar, L/D= 2.5, A/F= 30 Kg_{air}/Kg_{fuel}.

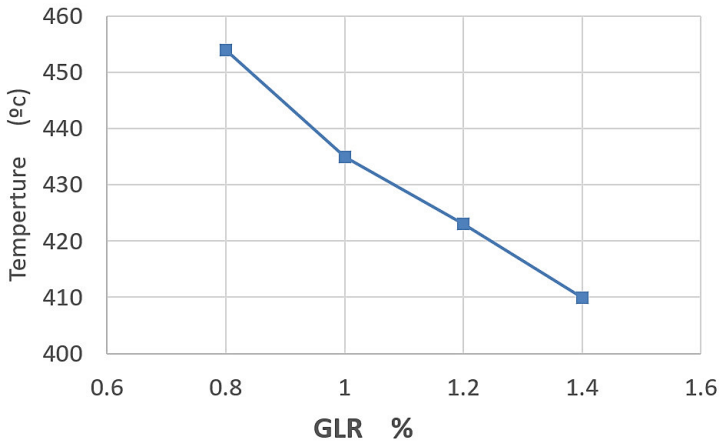

Figure 11. Stack temperature at different gas to liquid ratio at p_{inj} = 1.5 bar, L/D= 2.5, A/F= 30 Kg_{air}/Kg_{fuel}.

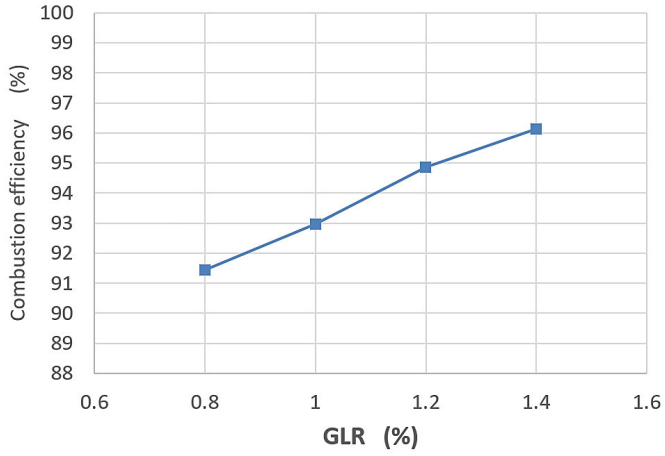

Figure 12. Combustion efficiency at different gas to liquid ratio at p_{inj} = 1.5 bar, L/D= 2.5, A/F= 30 Kg_{air}/Kg_{fuel}.

3.3 Influence of Injection Pressure

The injection pressure is an important operating parameter in most applications since it is desirable to minimize the amount of pressurized gas supplied while maintaining a small mean drop size. In this section the effect of injection pressure (p_{inj}) will be discussed in detail on flame temperature distribution, heat transfer to the cooling water and combustion efficiency.

3.3.1 Flame temperature distribution

The temperature distribution along the axis of the furnace for different values of injection pressures ranging from 0.5 to 2 bar are shown in Figure 13. While the A/F ratio and orifice diameter are kept constant and equal to 40, 2mm respectively. It is found that the temperature profile in all cases increases to the maximum temperature then decreases with moving downstream from the burner tip. It is shown that the maximum temperature of the flame is monitored between 15% – 25 % relative to furnace length from the atomizer tip at the different injection pressures, at which the mixing of air and fuel were nearly completed. As the injection pressure increases, the flame temperature increases in the flame region near the atomizer tip because of a good atomization and good mixing in this region and high reaction rate. In case of lower values of injection pressure, lower atomization degree is obtained and this leads to slow burning rate.

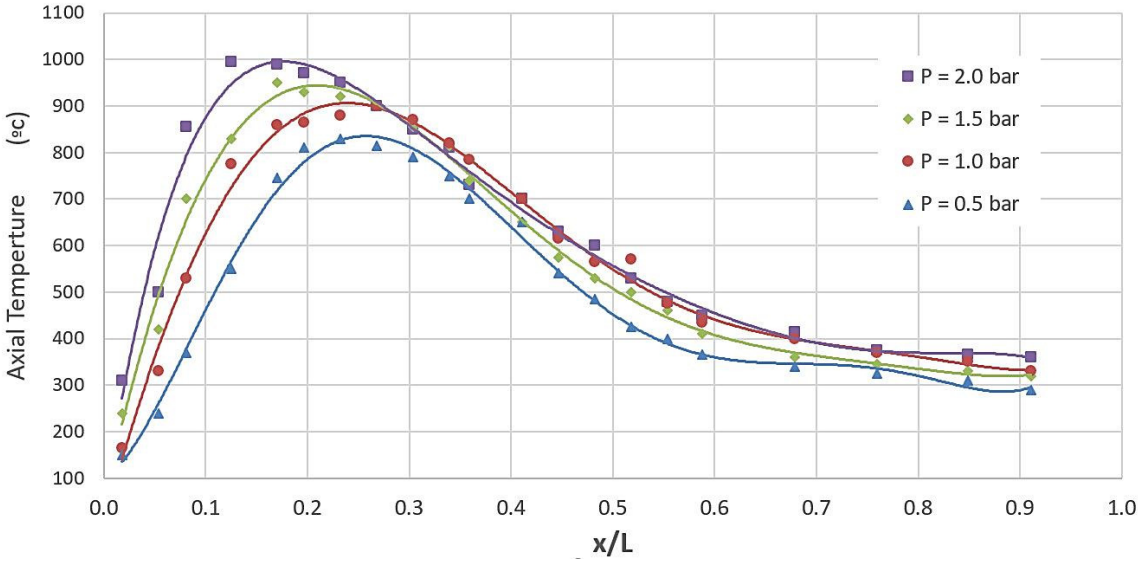

Figure 13. Influence of injection pressure on flame temperature distribution along the axis at A/F= 40 Kg_{air}/Kg_{fuel}, GLR= 1 %, and L/D = 2.5

Figure 14(a-d) illustrates 3-D surface of flame temperature in the combustor at different injection pressure ranging from 0.5 bar to 2 bar, A/F= 40 kg_{air}/Kg_{fuel} and exit orifice diameter 2 mm. It can be seen that the flame length decreases with increasing injection pressure and the maximum temperature moves toward burner tip. As the axial distance increases from the burner tip, the fuel mass flux become more uniform. Subsequently, the temperature distribution become more uniform and flatter. At the end of furnace, the temperature difference disappear because of the measuring points are outside the flame zone.

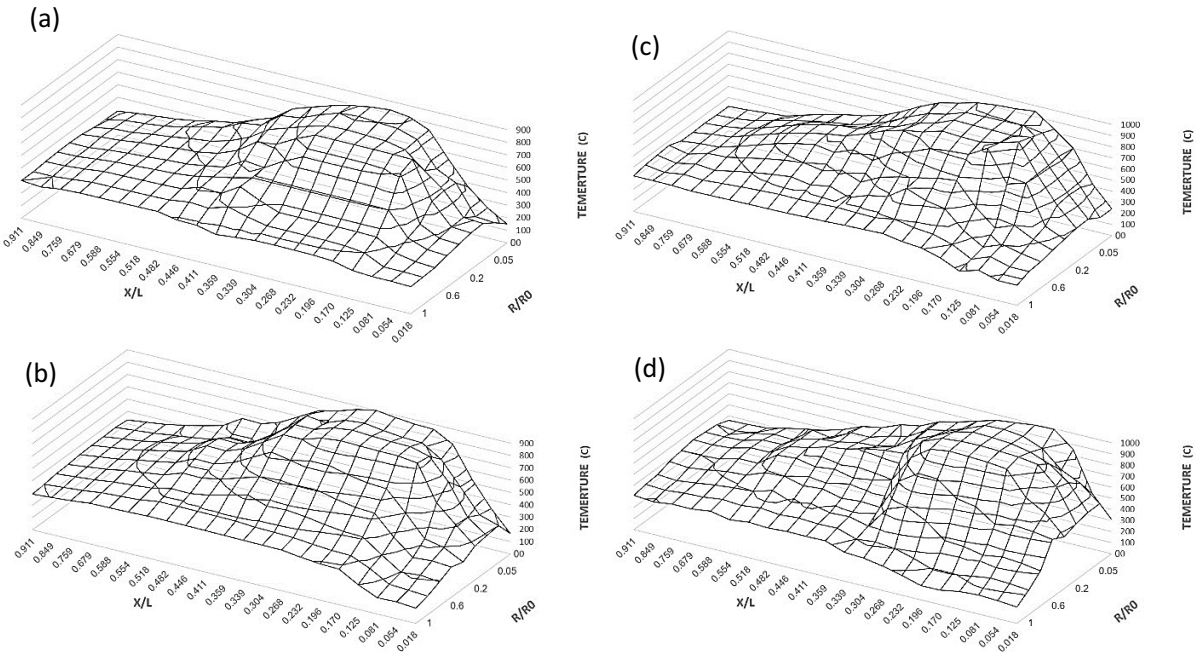

Figure 14. 3-D surface of flame temperature (°c) in the combustor at GLR= 1 %, L/D= 2.5, and A/F= 40 Kg_{air}/Kg_{fuel} a) p_{inj} = 0.5 bar b) p_{inj} =1 bar c) p_{inj} =1.5 bar d) p_{inj} =2 bar.

3.3.2 Cooling Water Heat Flux

Figure 15 shows that the heat flux to the water jacket as a function of injection pressures. It can be considered that, decreasing the injection pressure, leads to an increase in the amount of heat transferred to the cooling water jacket. This behavior can be interpreted as the increasing of injection pressure increases the spray axial velocity. Therefore, the higher injection pressure increases the rate of heat transfer at the furnace exit. Exhaust gases temperature give an indication of that behavior.

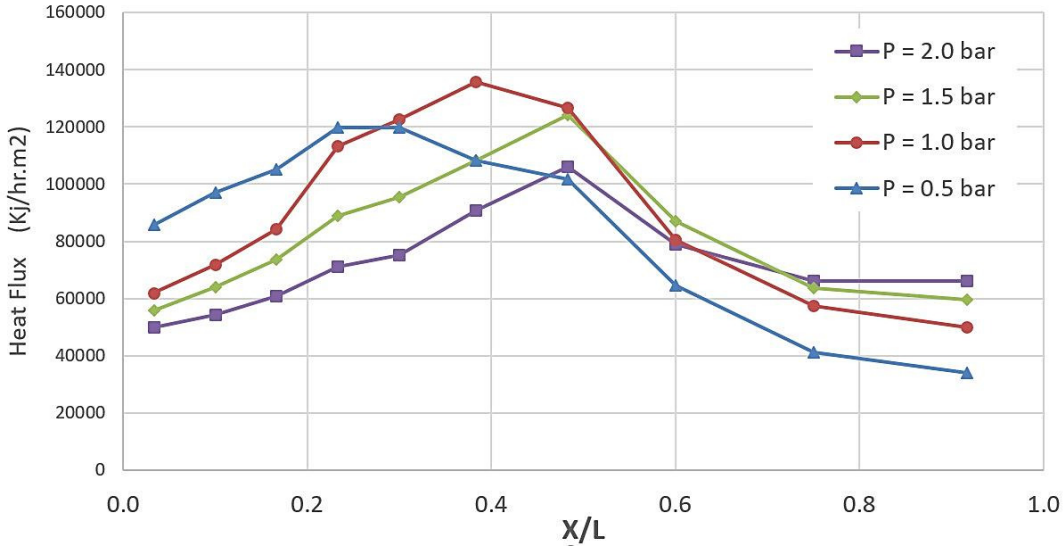

Figure 15. Total heat flux to the water jacket for different injection pressure at GLR = 1 %, L/D= 2.5, A/F= 40 Kg_{air}/Kg_{fuel}.

3.3.3 Stack Temperature

The exhaust gas temperatures at different values of injection pressure are illustrated in Figure 16. It is observed that the exhaust gas temperature increases with increasing the injection pressure. The main reason of this behavior is that the increasing of injection pressure increases the axial velocity of the spray. Moreover, the flame temperature distribution in the combustor and higher heat flux at last segment of cooling water give an indicate of higher exhaust gas temperature.

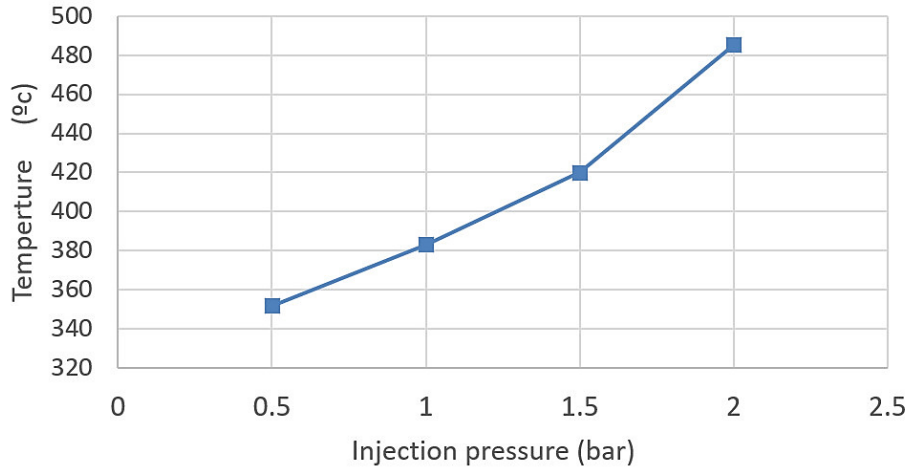

Figure 16. Stack temperature at different injection pressure at GLR= 1 %, L/D= 2.5, A/F= 40

3.3.4 Combustion Efficiency

Figure 17 shows the influence of injection pressure on combustion efficiency. The increasing of injection pressure increases the spray cone angle. This increasing of injection provides spray with fine drops and higher evaporating rate of the drops due to the higher turbulence of the air achieving good combustion with short stable flame. Therefore, the combustion efficiency increases at higher injection pressure. At higher A/F ratio, increasing of injection pressure more than 1 bar increases the combustion efficiency slowly. The higher combustion efficiency the lower pollutant emissions.

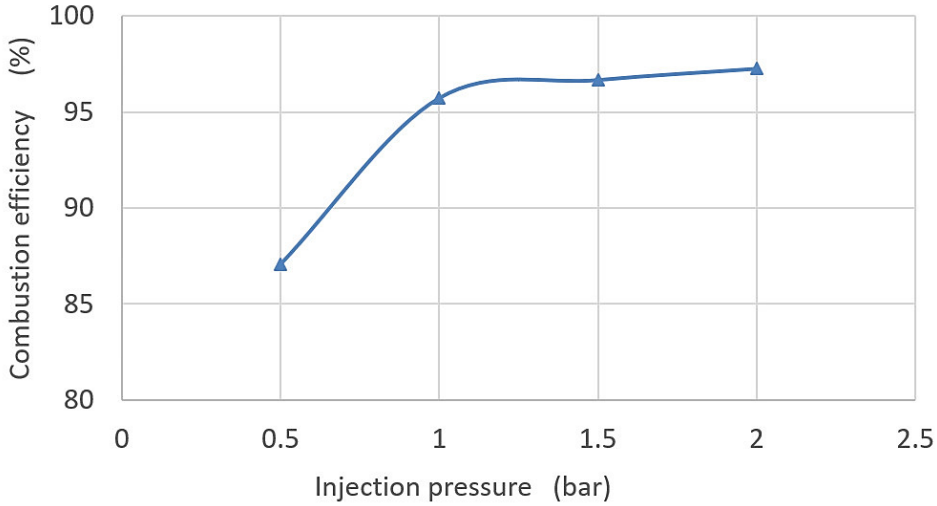

Figure 17. Influence of injection pressure on combustion efficiency at GLR = 1 %, L/D= 2.5, A/F= 40 Kg_{air}/Kg_{fuel}.

3.4 Influence of Exit Orifice Length to Diameter Ratio (L/D)

3.4.1 Flame temperature distribution

The flame temperature distribution along the axis of the flame for different (L/D) ratios at constant A/F = 40 Kg_{air}/Kg_{fuel}, p_{inj} =1.5 bar, and GLR= 1 % are shown in Figure 18. The small exit orifice diameter achieves good atomization. That leads to rapid evaporation of fuel and higher combustion rate and higher flame temperature. The decreasing of (L/D) ratio decreases the flame length and widen the spray cone angle. Therefore, the decreasing of (L/D) ratio shifting the maximum flame temperature towards the burner tip. It is found also that the maximum temperature of the flame is occurred at 20 % relative to furnace length, at which the mixing of air and fuel is nearly stoichiometric mixture and the rate of reaction is relatively high.

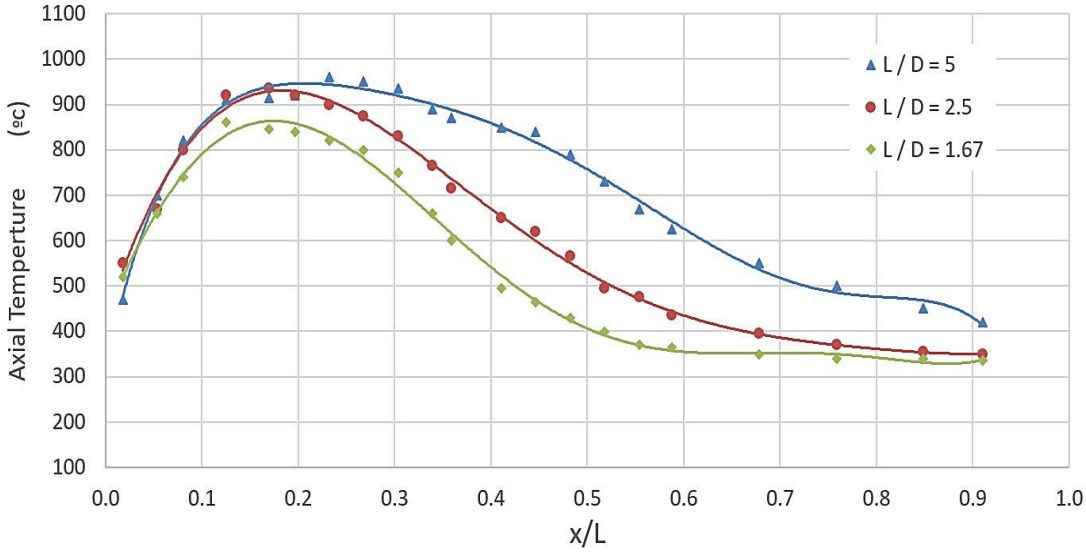

Figure 18. Influence of (L/D) ratio on flame temperature distribution along the axis at A/F= 40 Kg_{air}/Kg_{fuel}, GLR= 1 %, and p_{inj} = 1.5 bar.

Figure 19(a-c) shows 3-D surface of flame temperature in the combustor at different (L/D) ratios. It can be seen that the flame length increases with increasing (L/D) ratio and the maximum temperature moves to burner tip. All figures show nearly similar trend of the radial temperature profiles at different axial locations along the combustor. The profile near the burner tip shows a high

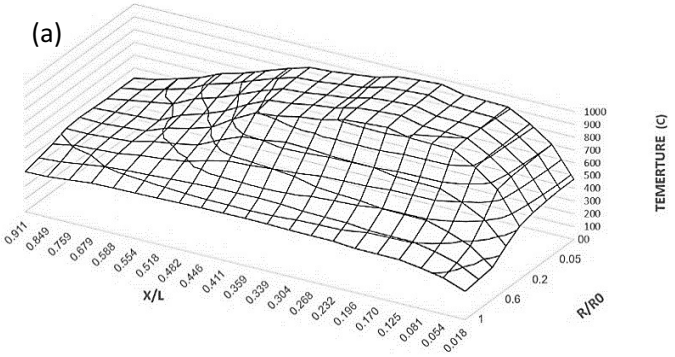

temperature at the flame zone and then a very low temperature at the other points outside the flame boundary. A uniform temperature region almost occurs in the outer recirculation zone and the temperature declines outside the flame boundary. Moving downward, the temperature profile becomes flat because of the measuring points lie outside the flame zone.

3.4.2 Cooling Water Heat Flux

Figure 20 shows heat flux for different values of (L/D) ratios. It is found that the heat flux profile in all cases increases to the maximum value then decreases with moving downstream from the burner tip. There is a good agreement between the temperature distribution in the combustor and the distribution of heat flux. The decreasing of (L/D) ratio decreases the flame length and widen the flame. Therefore, the rate of heat transfer to the cooling water increases near the burner tip then deceases at furnace exit because of decreasing flame temperature.

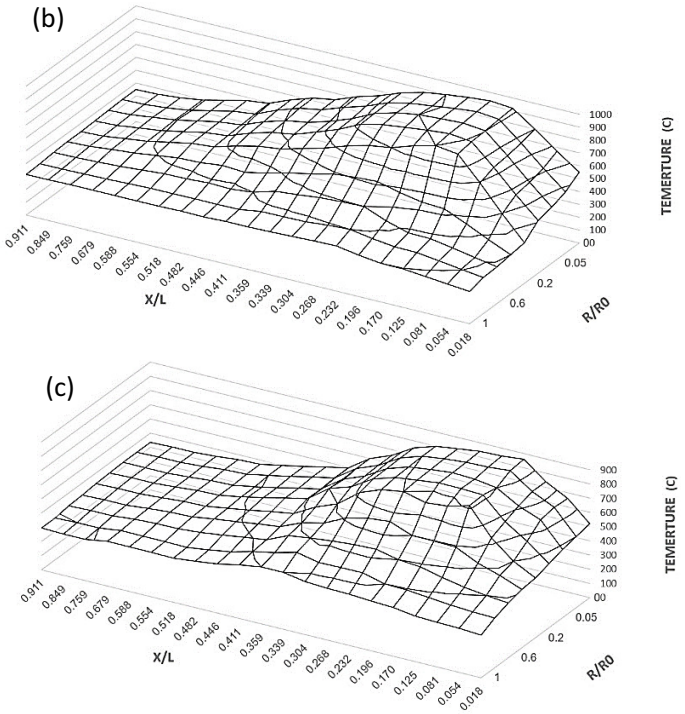

Figure 19. 3-D surface of flame temperature (°c) in the combustor at GLR= 1 %, A/F= 40 Kg_{air}/Kg_{fuel}, and p_{inj} = 1.5 bar a) L/D= 5 b) L/D= 2.5 c) L/D= 1.67

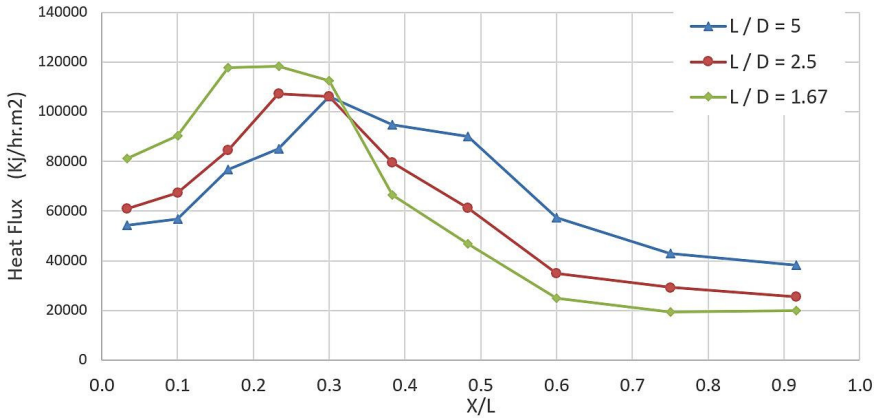

Figure 20. Total heat flux to the water jacket for different (L/D) ratio at GLR= 1 %, A/F= 40 Kg_{air}/Kg_{fuel}, and p_{inj} = 1.5 bar.

3.4.3 Stack Temperature

Figure 21 shows the exhaust gas temperatures at different values of (L/D) ratios. It is observed that the exhaust gas temperature increases with increasing (L/D) ratio. The main reason of this behavior is that the increasing of (L/D) ratio increases the flame length. Moreover, the flame temperature distribution in the combustor give an indication of higher exhaust gas temperature.

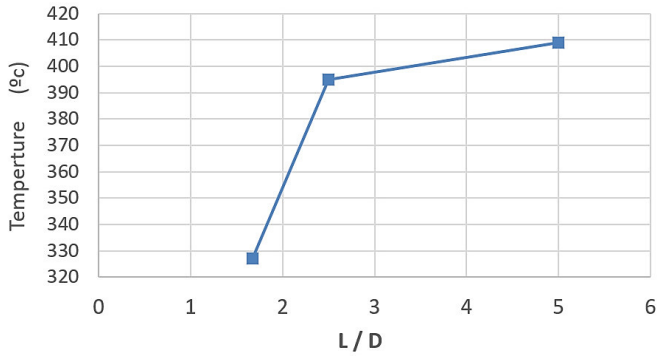

Figure 21. Stack temperature at different injection pressure at GLR= 1 %, and p_{inj} = 1.5 bar.

3.4.4 Combustion Efficiency

Figure 22 shows the influence of (L/D) ratio on combustion efficiency. The increasing of (L/D) ratio providing spray with fine drops and higher evaporating rate of the drops achieving combustion with short stable flame. Therefore, the combustion efficiency increases with using small exit orifice diameter. The higher combustion efficiency achieves low emissions because of The combustion efficiency is related to the amount of (UHC) and (CO).

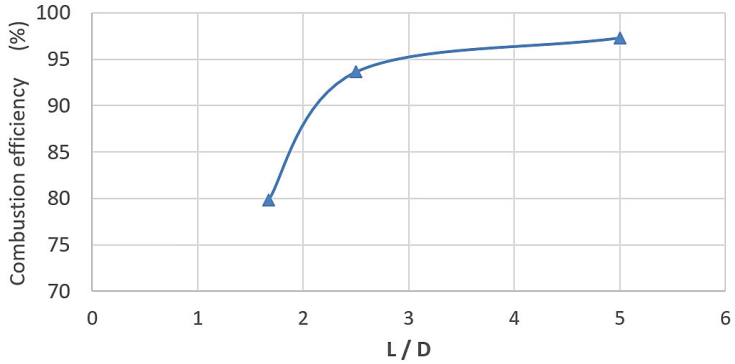

Figure 22. Influence of (L/D) ratio on combustion efficiency at GLR= 1 %, and p_{inj} = 1.5 bar.

4. Conclusion

In the present study, the spray and combustion characteristics produced by an effervescent atomizer is investigated experimentally for achieving clean combustion with high efficiency. The effects of air to fuel ratio, injection pressure, gas to liquid ratio, and exit orifice dimensions on the spray atomization and combustion characteristics are studied. From the obtained results, the important conclusions can be summarized as follows:

1. The flame temperature profile in all cases starts with a low temperature and increases rapidly to the maximum temperature then decreases with moving downstream from the burner tip. the maximum temperature of the flame lies in range of 15% to 20 % relative to furnace length. The maximum temperature moves toward burner tip with increasing A/F ratio, GLR, and injection pressure.
2. The increasing of injection pressure from 0.5 to 2 bar, GLR, and air to fuel ratio decreasing the flame length and providing clean combustion. The stack temperature decreases with increasing of gas to liquid ratio (GLR), exit orifice dimeter, and air to fuel ratio (A/F).
3. There is a clear similarity between the temperature distribution in the combustor and the distribution of cooling water heat flux.

4. The combustion efficiency increases at higher air to fuel ratios. At A/F ratio higher than 30 Kg_{air}/Kg_{fuel} the combustion efficiency is over 90%. The increasing of injection providing spray with fine drops and higher evaporating rate. Therefore, the combustion efficiency increases with increasing injection pressure from 0.5 to 2 bar. The combustion efficiency at injection pressure 1 bar(g) is higher than 95% at A/F ratio 40 Kg_{air}/Kg_{fuel}.

5. References

1) Lefebvre, A. H., X. F. Wang, and C. A. Martin. "Spray characteristics of aerated-liquid pressure atomizers." Journal of Propulsion and Power 4.4 :293-298, 1988.
2) Loebker, David W., and Howard Louis Empie Jr. "High mass flowrate effervescent spraying of a high viscosity Newtonian liquid." Proceedings of the 10th Annual Conference on Liquid Atomization and Spray Systems, 1997.
3) Lefebvre, A. "Atomization and sprays", hemisphere publishing corporation. New York, 1989.
4) Lian-sheng, L., Hua, Y., Xiang, G., Runze, D., & Yan, Y. "Experimental investigations on the spray combustion produced by effervescent atomizers." In Computer Distributed Control and Intelligent Environmental Monitoring (CDCIEM), International Conference on (pp. 305-311). IEEE, 2012.
5) Rehman, S., and K. Zaidi. "Design and fabrication of the high-pressure effervescent spray combustion system." International Journal 1: 72-77, 2014.
6) Y. Onuma and M. Ogasawara, "Studies on a spray combustion flame," in Symposium (International) on Combustion, vol. 15, no. 1, pp. 453–465, 1975.
7) Okasha, Gassan. "Diesel fuel and olive-cake slurry: atomization and combustion performance." Applied energy54.4: 315-326, 1996.
8) Khalid, A., Suardi, M., Chin, R. Y. S., & Amirnordin, S. H. "Effect of biodiesel-water-air derived from biodiesel crude palm oil using premix injector and mixture formation in burner combustion." Energy Procedia, 111, 877-884, 2017.
9) C. Pereira, G. Wang, and M. Costa, "Combustion of biodiesel in a large-scale laboratory furnace," Energy, vol. 74, pp. 950–955, 2014.
10) Akinyemi, Oladapo S., Lulin Jiang, and Jacob Bruno. "Effect of Fuel Properties and Atomizing Air to Liquid Ratio on Combustion Performance of a Novel Twin-Fluid Injector.", 2018.
11) Jiang, Lulin, Ajay K. Agrawal, and Robert P. Taylor. "Clean combustion of different liquid fuels using a novel injector." Experimental Thermal and Fluid Science 57: 275-284, 2014.
12) Sonar, D., Soni, S. L., Sharma, D., Srivastava, A., & Goyal, R." Performance and emission characteristics of a diesel engine with varying injection pressure and fueled with raw mahua oil (preheated and blends) and mahua oil methyl ester." Clean Technologies and Environmental Policy, 17(6), 1499-1511, 2015.
13) Brijesh, P., A. Chowdhury, and S. Sreedhara. "Advanced combustion methods for simultaneous reduction of emissions and fuel consumption of compression ignition engines." Clean Technologies and Environmental Policy 17.3: 615-625, 2015.
14) Lyons, Valerie J., and Richard W. Niedzwiecki. "Combustor technology for future small gas turbine aircraft.", 1993.
15) Noor MM, Wandel AP, Yusaf T. "Design and development of MILD combustion burner." Journal of Mechanical Engineering and Sciences.;5:662-76, 2013.
16) Noor MM, Wandel AP, Yusaf T. "The simulation of biogas combustion in a MILD burner." Journal of Mechanical Engineering and Sciences.;6:995-1013, 2014.
17) Gharehghani A, Hosseini R, Yusaf T. "Investigation of the effect of additives to natural gas on heavy-duty SI engine combustion characteristics." Journal of Mechanical Engineering and Sciences.;5:677-87, 2013.
18) Kamil M, Rahman MM, Bakar RA. "Performance evaluation of external mixture formation strategy in hydrogen fueled engine." Journal of Mechanical Engineering and Sciences.;1:87-98, 2011.
19) Noor M, Wandel AP, Yusaf T. "MILD combustion: the future for lean and clean combustion." International Review of Mechanical Engineering.;8:251-7, 2013.